Volume 1
Number 1
January 2023
Pages 1–168

RSC Sustainability

rsc.li/rscsus

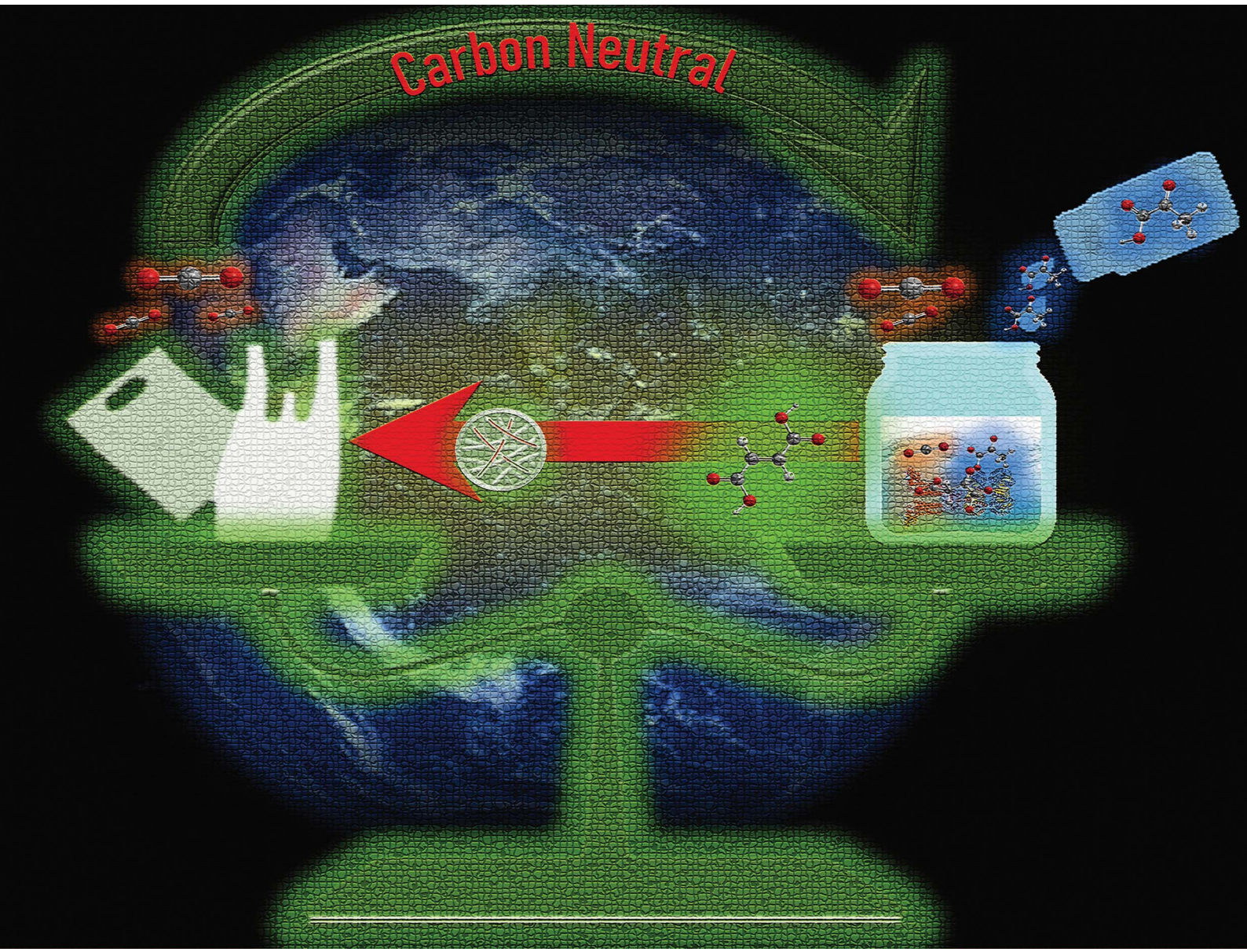

ISSN 2753-8125

ROYAL SOCIETY OF CHEMISTRY

PAPER

Mika Takeuchi and Yutaka Amao
Phosphate-induced enhancement of fumarate production from a CO_2 and pyruvate with the system of malate dehydrogenase and fumarase

RSC Sustainability

ROYAL SOCIETY OF CHEMISTRY

PAPER

View Article Online
View Journal | View Issue

Cite this: *RSC Sustainability*, 2023, **1**, 90

Phosphate-induced enhancement of fumarate production from a CO_2 and pyruvate with the system of malate dehydrogenase and fumarase†

Mika Takeuchi[a] and Yutaka Amao *[ab]

Fumarate is a useful unsaturated dicarboxylate and utilized as a raw material for unsaturated polyester resin. As a fumarate is produced using a petroleum-derived material, thus, it is required to establish a synthesis from renewable raw materials such as CO_2 and biomass derived substances. In this work, the synthesis of fumarate from CO_2 and pyruvate in an aqueous medium using a multi-biocatalytic system of malate dehydrogenase (oxaloacetate-decarboxylating; ME; EC 1.1.1.38) from *Sulfobus tokodaii* and fumarase from porcine heart (FUM; EC 4.2.1.2) in the presence of NADH is established. In this system, it is important to improve the efficiency of fumarate production based on FUM-catalyzed dehydration of L-malate in aqueous media. It was found that saturation of the additional substrate binding site present in FUM with phosphate promotes fumarate production based on the dehydration of L-malate. Under the reaction condition of L-malate (1.0 mM) and FUM (1.3 nM) in HEPES buffer (pH 7.0) for fumarate production, the addition of 70 mM phosphate improved the fumarate production rate up to 2.4 times compared to no addition of phosphate. On the other hand, no effect of phosphate addition on the ME-catalyzed L-malate production from pyruvate and CO_2 in the presence of NADH was observed. In particular, the conversion yield for pyruvate to fumarate with the system of ME and FUM was improved up to 1.6 times due to the improvement in the catalytic activity of FUM caused by the addition of phosphate in this system.

Received 27th August 2022
Accepted 19th October 2022

DOI: 10.1039/d2su00031h

rsc.li/rscsus

Sustainability spotlight

This research is to synthesize raw materials of biodegradable polymers from CO_2 and biomass-derived molecules using multi-biocatalysts in aqueous media under mild conditions compared with the conventional industrial methods for the synthesis of raw materials of biodegradable polymers. Therefore, this research contributes to the CO_2 fixation, and to alternative plastic raw material production for sustainable society. This system can fix CO_2 in organic molecules and convert them into high-value-added materials, resulting in long-term storage of CO_2 in molecules. This work aligns with the goals 7 of "Affordable and Clean Energy" and 12 of "Responsible Consumption and Production" in the UN's Sustainable Development Goals.

Introduction

An unsaturated dicarboxylic acid, fumaric acid is used in the production of polyester resins.[1–5] In recent years, a synthetic method using fumaric acid as a raw material for poly (butylene succinate) (PBS), as a biodegradable plastic with a low environmental impact, has attracted attention.[6–8] An industrial fumaric acid production requires furfural oxidation using chlorate with a vanadium oxide catalyst. In this process, the reaction temperature is 70–100 °C and some harsh reaction conditions are required.[9] Therefore, fumaric acid is produced using petroleum-derived materials, and it is required to establish a synthesis method from renewable raw materials such as CO_2 and biomass derived substances in the future. In view of such restrictions on the use of fossil resources, we resorted to a biocatalytic method for synthesizing fumaric acid from CO_2 and biomass derived substances. We focused on the use of malate dehydrogenase (NAD^+-dependent oxaloacetate-decarboxylating) (malic enzyme; ME EC 1.1.1.38)[10,11] and fumarase (FUM; EC 4.2.1.2)[12–17] in the tricarboxylic acid cycle (TCA cycle) with a series of the biological important chemical reactions to release stored energy for aerobic metabolism.[18–22] Achievement of technology using solar light energy in addition to a biomass-derived substance, CO_2, will lead to innovative fumarate synthesis. We are planning to develop the visible-light driven fumarate production from pyruvate and CO_2 with the combination of the NAD^+ reduction system of an electron donor (D), a photosensitizer (PS) and a catalyst such as colloidal Rh nanoparticles or a Rh coordination complex ($[Cp^*Rh(bpy)(H_2O)]^{2+}$;

[a]*Graduate School of Science, Osaka Metropolitan University, 3-3-138 Sugimoto, Sumiyoshi-ku, Osaka 558-8585, Japan*

[b]*Research Centre of Artificial Photosynthesis (ReCAP), Osaka Metropolitan University, 3-3-138 Sugimoto, Sumiyoshi-ku, Osaka 558-8585, Japan. E-mail: amao@omu.ac.jp*

† Electronic supplementary information (ESI) available. See DOI: https://doi.org/10.1039/d2su00031h

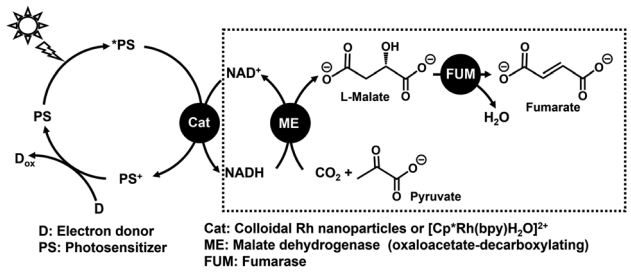

Fig. 1 Visible-light driven fumarate production from pyruvate and CO_2 with the system of an electron donor (D), a photosensitizer (PS), a catalyst for NADH regeneration, ME and FUM.

Cp* = pentamethylcyclopentadienyl, bpy = 2,2′-bipyridyl),[23–34] and multi-biocatalysts (ME and FUM) as shown in Fig. 1.

The fumarate synthesis from pyruvate and bicarbonate in an aqueous medium using ME and FUM in the presence of NADH (the process in the dotted line in Fig. 1) was reported previously. As the process of ME-catalyzed L-malate production from pyruvate and CO_2 throughout the reaction leads to improved fumarate production, the reaction conditions that optimize ME-catalyzed pyruvate carboxylation with CO_2 and the effects of metal ion cofactor for ME on FUM-catalyzed fumarate production were clarified.[35] Moreover, ME also has a lactate dehydrogenase function and catalyzes the reduction of pyruvate to lactate in the presence of NADH. Lactate production with ME is suppressed by adding excess amount of CO_2 or bicarbonate.[36] This indicates that the carboxylation of pyruvate can be preferentially catalyzed using ME with an excess of CO_2 or bicarbonate. By using the optimized system, the conversion yield for pyruvate to fumarate with the system of ME and FUM in the presence of NADH was estimated to be 7.0%.[35] In contrast, the unique ability of FUM to dehydrate the hydroxyl groups of organic molecules to form C–C unsaturated bonds in an aqueous medium allows green catalytic reactions to be achieved without the use of organic solvents. However, previous reports have not yet achieved optimization of the FUM-catalyzed dehydration process of L-malate to fumarate.[36] In order to further improve the overall fumarate production yield, it is necessary to efficiently dehydrate the hydroxyl-group of L-malate in an aqueous medium.

In this study, focusing on the subunit structure of FUM, we attempted to improve the production of fumarate based on the dehydration of L-malate by saturating the additional substrate binding site of FUM with an inorganic salt. Also, the improvement of conversion yield for pyruvate and CO_2 to fumarate with the system of ME and FUM was attempted due to the enhancement in the catalytic activity of FUM caused by the addition of the inorganic salt in this system.

Experimental

Materials

Malate dehydrogenase decarboxylating type (ME, EC 1.1.1.38 code: MDH-73-01 obtained from *Sulfobus tokodaii*; commercially available reagent, 14 mg mL^{-1}; 0.55 units per mg) was purchased from Thermostable Enzyme Laboratory Co., Ltd. One activity unit of ME converts 1.0 μmol of NADH to NAD^+ in the presence of 10 mM sodium pyruvate, 0.3 mM NADH, 10 mM sodium bicarbonate and 10 mM magnesium chloride in 50 mM 1,4-piperazinediethanesulfonic acid-KOH buffer per min at pH 6.5 at 37 °C according to the data sheet provided by Thermostable Enzyme Laboratory Co., Ltd. The molecular weight of ME was estimated to be 40 kDa based on the SDS-page using electrophoresis. Fumarase (FUM) from porcine heart (EC 4.2.1.2; molecular weight: 200 kDa)[37,38] was purchased from Merck Co., Ltd. One activity unit of FUM converts 1.0 μmol of L-malate to fumarate in potassium phosphate buffer per min at pH 7.6 at 25 °C. NADH was supplied by Oriental Yeast Co. Ltd. 4-(2-Hydroxyethyl)-1-piperazineethanesulfonic acid (HEPES) was purchased from Nacalai Tesque, Inc. (Kyoto, Japan). The other chemicals were of analytical grade or the highest grade available purchased from Wako Pure Chemical Co. Ltd.

pH Dependence of FUM catalyzed fumarate production from L-malate

The reaction was started by adding FUM (0.5 units; 1.3 nM) to the solution of sodium L-malate (1.0 mM) in 5.0 mL of 500 mM HEPES buffer with the thermostatic chamber set at a temperature of 30.5 °C. The pH of the sample solution was varied from 6.3 to 8.6. The reaction vessel is a clear glass vial, and the reaction is a sealed system. The total volume of the reaction vessel is 11.0 mL. The amount of fumarate produced was detected using an ion chromatography setup (Metrohm, Eco IC; electrical conductivity detector) with an ion exclusion column (Metrosep Organic Acids 250/7.8 Metrohm; column size: 7.8 × 250 mm; composed of 9 μm polystyrene-divinylbenzene copolymer with sulfonic acid groups). Details of L-malate and fumarate quantification by ion chromatography are described in the ESI.† The L-malate and fumarate concentrations were determined from the calibration curve based on the chromatogram of a standard sample (Fig. S2(a) and (b)†) as shown in Fig. S3(a) and (b)† using eqn (S1) and (S2).†

Effect of phosphate on the FUM catalyzed fumarate production from L-malate

The reaction was started by adding FUM (0.5 units; 1.3 nM) to the solution of sodium L-malate (1.0 mM) and phosphate (0–100 mM) in 5.0 mL of 500 mM HEPES buffer (pH 7.0) in a thermostatic chamber set at a temperature of 30.5 °C. The reaction vessel is a clear glass vial, and the reaction is a sealed system. The total volume of the reaction vessel is 11.0 mL. The amount of fumarate produced was detected by ion chromatography. In order to prevent the pH fluctuation of the sample solution due to the addition of phosphate, sodium dihydrogen phosphate and disodium hydrogen phosphate were used to maintain the pH at 7.0.

Effect of phosphate on the ME catalyzed L-malate production from pyruvate and CO_2 in the presence of NADH

The reaction mixture consisted of sodium pyruvate (5.0 mM), NADH (5.0 mM), magnesium chloride (5.0 mM), sodium

bicarbonate (100 mM) and phosphate (0–100 mM) in 5.0 mL of 500 mM CO_2 saturated HEPES buffer (pH 7.0). The reaction vessel is a clear glass vial, and the reaction is a sealed system. The total volume of the reaction vessel is 11.0 mL. The gas phase of the reaction vessel and sample solution were replaced by flowing CO_2 gas at a flow rate of 0.1 L min^{-1} for 10 min. In order to prevent the pH fluctuation of the sample solution due to the addition of phosphate, sodium dihydrogen phosphate and disodium hydrogen phosphate were used to maintain the pH at 7.0. The reaction was started by adding ME (0.7 units; 6.5 μM) to the above mixture in a thermostatic chamber set at a temperature of 30.5 °C. The amount of L-malate produced was detected by ion chromatography. Details of pyruvate quantification by ion chromatography are described in the ESI.† The pyruvate concentration was determined from the calibration curve based on the chromatogram of a standard sample (Fig. S4(a)) as shown in Fig. S4(b) using eqn (S3).†

Effect of phosphate on the ME and FUM catalyzed fumarate production from pyruvate and CO_2 in the presence of NADH

The reaction mixture consisted of sodium pyruvate (5.0 mM), NADH (5.0 mM), magnesium chloride (5.0 mM), sodium bicarbonate (100 mM) and phosphate (0–100 mM) in 5.0 mL of 500 mM CO_2 saturated HEPES buffer (pH 7.0). The reaction vessel is a clear glass vial, and the reaction is a sealed system. The total volume of the reaction vessel is 11.0 mL. The gas phase of the reaction vessel and sample solution were replaced by flowing CO_2 gas at a flow rate of 0.1 L min^{-1} for 10 min. In order to prevent the pH fluctuation of the sample solution due to the addition of phosphate, sodium dihydrogen phosphate and disodium hydrogen phosphate were used to maintain the pH at 7.0. The reaction was started by adding the mixture of ME (0.7 units; 6.5 μM) and FUM (0.5 units; 1.3 nM) to the above mixture in a thermostatic chamber set at a temperature of 30.5 °C. The amount of L-malate and fumarate produced was detected by ion chromatography.

Results and discussion

pH Dependence of FUM catalyzed fumarate production from L-malate

Fig. 2 shows the pH dependence on the initial rate of fumarate production (v_0) with the system of sodium L-malate and FUM in HEPES buffers with varying pH from 6.3 to 8.6. The reason for changing the pH of the reaction solution from 6.3 to 8.6 is as follows. It is predicted that the FUM-catalyzed dehydration of L-malate to produce fumarate requires a base such as the hydroxide ion. Therefore, acidic, neutral and basic conditions were selected as the varying pH values of the reaction solution for the FUM-catalyzed dehydration of L-malate. The initial reaction rate was calculated from the concentration of fumarate produced after 5 min of incubation. As shown in Fig. 2, the v_0 of fumarate production was maximized around pH 7.0 of the reaction solution. In contrast to expectations, a tendency for v_0 to decrease was observed under the basic conditions compared to at pH 7.0. The cause of the decrease in the rate of fumarate

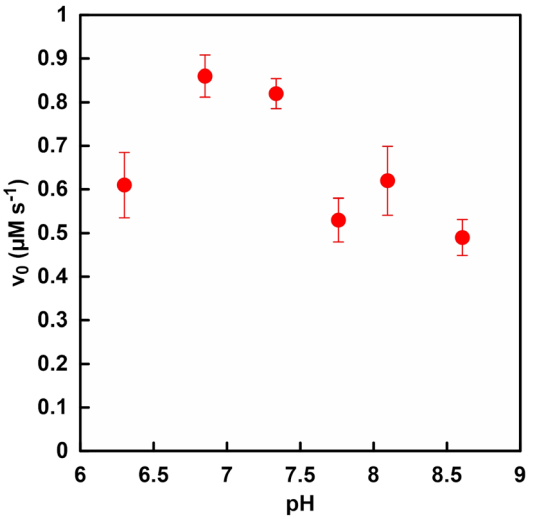

Fig. 2 The pH dependence on the initial rate of fumarate production (v_0) with the system of sodium L-malate and FUM in HEPES buffer with varying pH from 6.3 to 8.6. Each plot shows the mean error of multiple measurements.

production under basic conditions has not yet been clarified. However, one of the possible reasons is that elimination of the hydroxide ion from the intermediate produced in the process of fumarate production from L-malate was prevented. Since v_0 decreased even under acidic conditions, the other possible reason is that the pH-dependent conformational change of FUM may cause decrease in the rate of fumarate production. From these results, the optimum pH for fumarate production based on FUM-catalyzed dehydration of L-malate was determined to be 7.0. Moreover, the optimum pH for ME catalyzed L-malate production due to the pyruvate carboxylation of CO_2 also was observed to be around 7.0.[35] Therefore, the pH of the reaction system using FUM and ME for fumarate production from pyruvate and CO_2 was adjusted to 7.0.

Effect of phosphate on the FUM catalyzed fumarate production from L-malate

Next, the improvement of the efficiency of fumarate production by adding a molecule that can act directly on the substrate binding site of FUM was attempted. It has been reported that FUM is a tetrameric enzyme consisting of four identical subunits of 50 kDa each.[37,38] There are two different substrate binding sites (sites A and B) with different affinities as shown in Fig. 3.[37] It has been reported that site A has catalytic activity, whereas site B has no catalytic activity.[38] The affinity of site B for substrates is 1–2 orders of magnitude lower than the affinity of site A. However, L-malate and fumarate bind to both sites A and B. It has been reported that saturating site B results in an increase in the overall activity of fumarase for the L-malate dehydration to fumarate.

An essential tyrosine residue was found to be located in site A; in contrast, an essential methionine residue resides in or near site B. Site A is composed of amino acid residues T100, S139, S140, N141, T187, H188, K324, and N326.[39] On the other

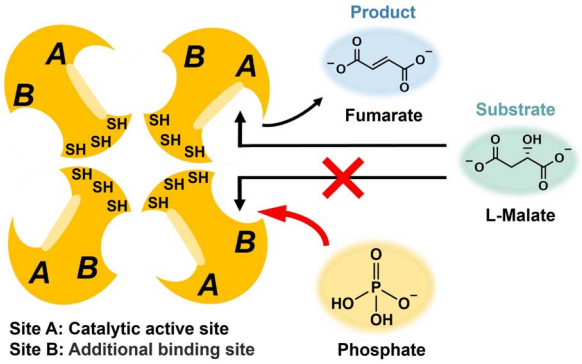

Fig. 3 Schematic representation of the model of tetramer of FUM.

hand, site B forms a π-helix between amino acid residues H129 and N135.[39] Different properties are observed due to the three-dimensional structure between the sites A and B.[39] For example, pyromellitic acid is indeed able to bind to sites A and B at the same time. Thus, pyromellitic acid functions as a competitive inhibitor of FUM-catalyzed L-malate dehydration to fumarate. On the other hand, it has been reported that sulfate easily binds to site B and has a function of saturating site B. However, excessive addition of sulfate causes FUM to precipitate in aqueous solution. Therefore, we investigated the effect of phosphate, a highly biocompatible oxoacid widely used as a buffer solution, on the conversion of FUM-catalyzed L-malate to fumarate. Saturation of site B of FUM with phosphate makes it possible to preferentially induce binding of L-malate to site A as shown in Fig. 3.

First, FUM-catalyzed dehydration-based fumarate production was attempted in 500 mM phosphate buffer (pH 7.0) instead of HEPES. However, no fumarate production was observed with incubation time. From this result it can be suggested that high concentrations of phosphate may inhibit FUM-catalyzed fumarate production. Therefore, the effect of phosphate concentration on FUM-catalyzed fumarate production in HEPES buffer was investigated. Fig. 4 shows a chart of an ion chromatogram sampled from the reaction solution in the presence of 70 mM of phosphate with incubation time as an example. The retention times for L-malate and fumarate were detected at 10.11–10.13 and 12.28–12.37 min, respectively. As shown in Fig. 4, signal peaks attributed to L-malate and fumarate decrease and increase with incubation time, respectively. This result indicates a FUM-catalyzed conversion of L-malate to fumarate.

Fig. 5 shows the time dependence of the concentration of fumarate production estimated from an ion chromatogram sampled from the reaction solution with the system of sodium L-malate and FUM in HEPES buffer containing various phosphate concentrations (0–100 mM). As shown in Fig. 5, the amount of fumarate produced increased with a phosphate concentration between 50 and 80 mM, but decreased with the addition of more than 80 mM of phosphate.

Fig. 6 shows the relationship between the rate of fumarate production (v) and incubation time.

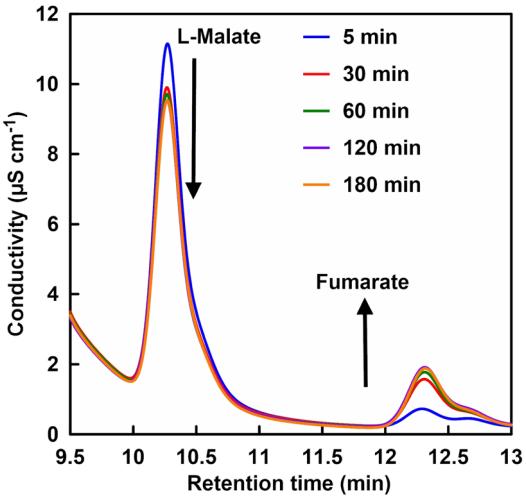

Fig. 4 A chart of an ion chromatogram sampled from the reaction solution containing L-malate, FUM and phosphate in HEPES buffer (pH 7.0).

It was suggested that the initial rate of fumarate production (after 5 min incubation) was significantly improved with a phosphate concentration between 50 and 80 mM as compared with that without phosphate. On the other hand, the initial rate of fumarate production under the phosphate concentration of 100 mM was lower than that without phosphate. This result is consistent with the inhibition of FUM-catalyzed conversion of L-malate to fumarate under conditions using 500 mM phosphate buffer. The substrate, L-malate, can bind to both sites A and B. Phosphate, on the other hand, has a structural similarity to the carbonyl group of L-malate, but does not have α-hydrogen, so it does not bind to the catalytic site A, but only to site B.

Therefore, owing to the coexistence of the phosphate in the reaction solution, the non-catalytic site B is occupied by the

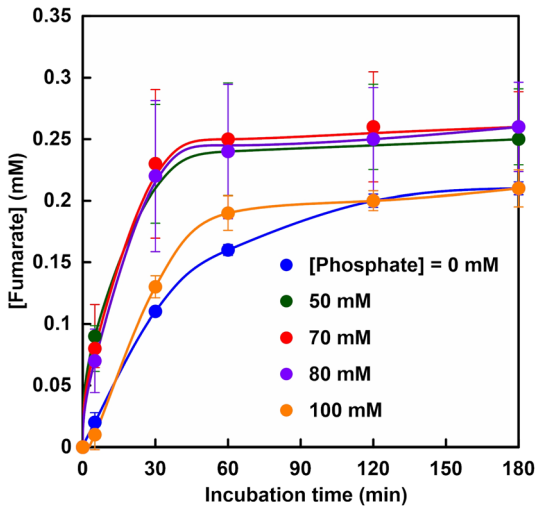

Fig. 5 Time course of fumarate production with the system of sodium L-malate and FUM in HEPES buffer (pH 7.0) containing various phosphate concentrations. Each plot shows the mean error of multiple measurements.

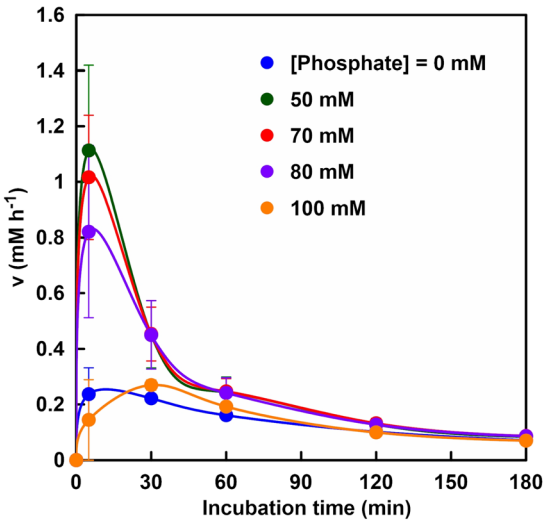

Fig. 6 Time dependence of the rate of fumarate production (v) with the system of sodium L-malate and FUM in HEPES buffer (pH 7.0) containing various phosphate concentrations. Each plot shows the mean error of multiple measurements.

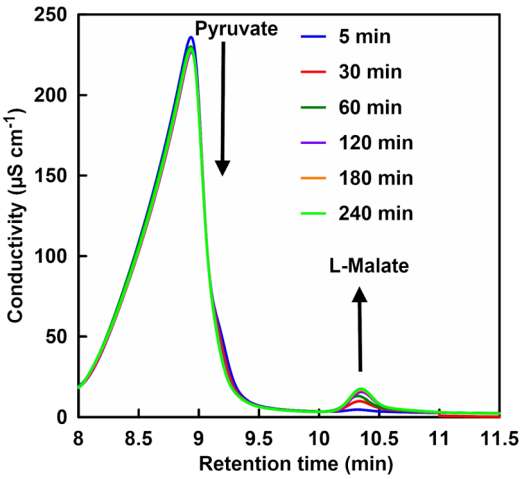

Fig. 7 A chart of an ion chromatogram sampled from the reaction solution containing sodium pyruvate, NADH, magnesium chloride, sodium bicarbonate and ME in CO_2 saturated HEPES buffer containing 70 mM phosphate.

phosphate, and the substrate L-malate preferentially binds to the catalytically active site (site A). Under the reaction condition of sodium L-malate (1.0 mM) and FUM (1.3 nM) in HEPES buffer (pH 7.0) for fumarate production, 70 mM phosphate is determined to be the optimum concentration. After 180 min incubation, the yield for L-malate to fumarate under the conditions of sodium L-malate (1.0 mM), FUM (1.3 nM) and phosphate (70 mM) in HEPES buffer (pH 7.0) was estimated to be 26 ± 3% and the turnover number of FUM for fumarate production was calculated to be *ca.* 1111 min^{-1}. Thus, it has been suggested that the addition of phosphate is effective for FUM-catalyzed conversion of L-malate to fumarate.

Effect of phosphate on the ME catalyzed L-malate production due to the pyruvate carboxylation of CO_2

Next, the effect of phosphate addition on the ME-catalyzed pyruvate carboxylation of CO_2 to produce L-malate was investigated. Fig. 8 shows a chart of an ion chromatogram sampled from the reaction solution in the presence of 70 mM of phosphate with incubation time as an example. The retention times for pyruvate and L-malate were detected at 8.71–9.20 and 10.11–10.13 min, respectively. As shown in Fig. 7, signal peaks attributed to pyruvate and L-malate decrease and increase with incubation time, respectively. Fig. 8 shows the time dependence of L-malate production with the system of sodium pyruvate, NADH, magnesium chloride, sodium bicarbonate and ME in CO_2 saturated HEPES buffer containing various phosphate concentrations.

As shown in Fig. 8, no change in L-malate production concentration with the system of sodium pyruvate, NADH, magnesium chloride, sodium bicarbonate and ME in CO_2 saturated HEPES buffer was observed by the addition of phosphate of 0–100 mM. Thus, it is suggested that phosphate addition does not affect L-malate production with the system of sodium pyruvate, NADH, magnesium chloride, sodium bicarbonate and ME.

Effect of phosphate on the ME and FUM catalyzed fumarate production from pyruvate and CO_2 in the presence of NADH

Finally, the effect of phosphate addition on the fumarate production system from pyruvate and CO_2 using ME and FUM was investigated. We reported that the Mg^{2+} (ME cofactor) affects the conversion of FUM-catalyzed L-malate to fumarate and the optimal concentration of Mg^{2+} for the pyruvate and CO_2 to fumarate production system using ME and FUM was determined to be 5.0 mM. In this system, thus, the Mg^{2+} concentration was adjusted to 5.0 mM. Fig. 9 shows a chart of an ion

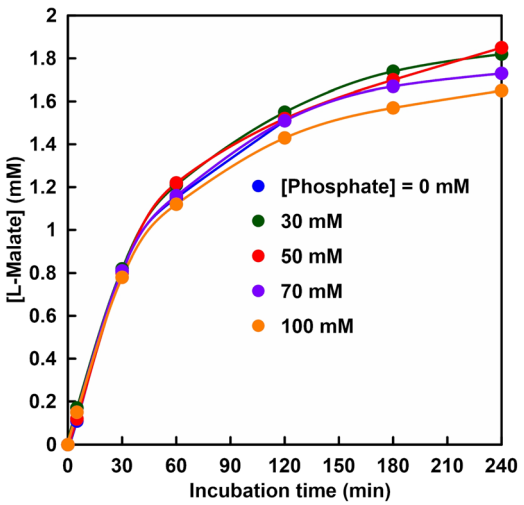

Fig. 8 Time course of L-malate production with the system of sodium pyruvate, NADH, magnesium chloride, sodium bicarbonate and ME in CO_2 saturated HEPES buffer containing various phosphate concentrations.

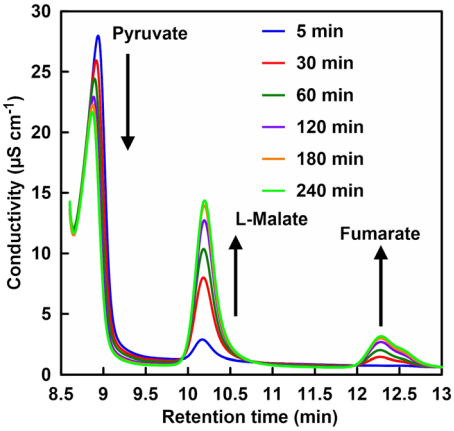

Fig. 9 A chart of an ion chromatogram sampled from the reaction solution containing sodium pyruvate, NADH, magnesium chloride, sodium bicarbonate, ME and FUM in CO_2 saturated HEPES buffer containing 10 mM phosphate.

chromatogram sampled from the reaction solution in the presence of 10 mM of phosphate with incubation time as an example.

The retention times for pyruvate, L-malate and fumarate were detected at 8.71–9.20, 10.11–10.13 and 12.28–12.37 min, respectively. As shown in Fig. 9, the signal peak attributed to pyruvate decreases with incubation time. In contrast, signal peaks attributed to L-malate and fumarate increase with incubation time.

Fig. 10 shows the time dependence of L-malate (a) and fumarate (b) production with the system of sodium pyruvate, NADH, magnesium chloride, sodium bicarbonate, ME and FUM in CO_2 saturated HEPES buffer containing various phosphate concentrations. As shown in Fig. 10, the amount of fumarate produced also increased up to a phosphate concentration of 70 mM, but decreased with the addition of more than 70 mM of phosphate in the system of sodium pyruvate, NADH, magnesium chloride, sodium bicarbonate, ME and FUM in CO_2 saturated HEPES buffer. After 240 min incubation, the fumarate concentration was estimated to be 0.55 ± 0.06 mM under the condition with 70 mM of phosphate. The yield for pyruvate to fumarate was estimated to be 11.0 ± 1.2%.

On the other hand, the yield for pyruvate to fumarate was reported to be 7.0% in the system with optimized Mg^{2+} concentration. In addition, when the effect of addition of other metal ions (Cu^{2+}, Fe^{2+}, Al^{3+}) other than Mg^{2+}, a co-factor of ME, to fumarate production based on dehydration of L-malate catalyzed by FUM was investigated, almost no effect was observed. From the above results it can be concluded that the addition of phosphate to this system can be an effective means of producing fumarate from pyruvate and bicarbonate with the system of ME and FUM in the presence of NADH.

The ME used in this system is classified as a thermostable enzyme, and it has been confirmed that it does not lose its enzymatic activity even at a reaction temperature of 60 °C. On the other hand, FUM from porcine heart is reported to have an optimum temperature of around 30 °C and does not exhibit

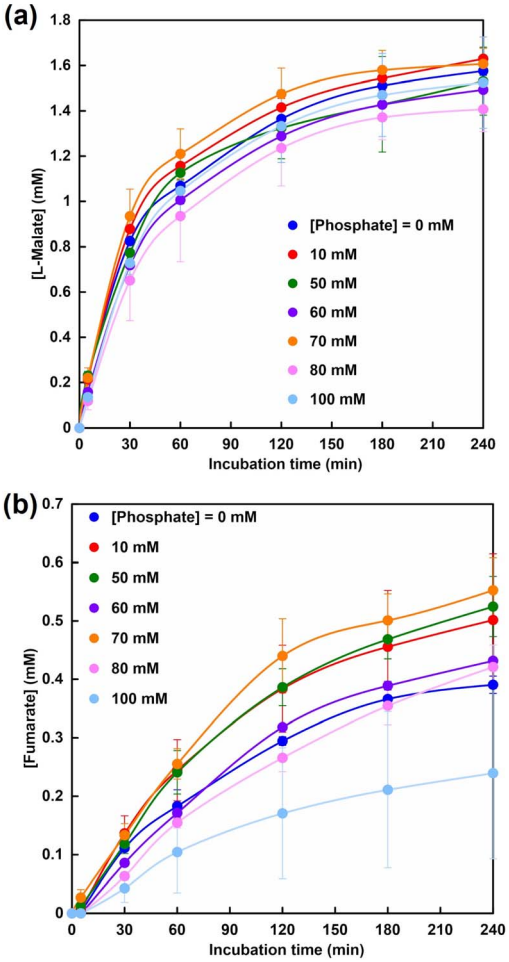

Fig. 10 Time course of L-malate (a) and fumarate (b) production with the system of sodium pyruvate, NADH, magnesium chloride, sodium bicarbonate, ME and FUM in CO_2 saturated HEPES buffer containing various phosphate concentrations. Each plot shows the mean error of multiple measurements.

heat resistance at 60 °C. In addition, since this system uses CO_2 as a reaction substrate in an aqueous solution, it transforms from the liquid into the gas phase due to the decrease in the solubility of CO_2 under high temperature conditions. Considering these conditions, the reaction temperature for fumarate production from pyruvate and CO_2 with ME and FUM was set at 30 °C.

Finally, let's discuss the stability and reusability of ME and FUM in this system. This system is a homogeneous catalyst system, and at present, it is not possible to retrieve ME and FUM from the sample solution after the reaction. Biocatalyst stabilization and recycling are important issues in the final application for practical usage. As a solution to these issues, there are some techniques for immobilizing the biocatalyst on a catalytic support.[40,41] By using the immobilization techniques, the biocatalyst is retrieved and reused for many cycles. We are currently investigating the co-immobilization of ME and FUM to metal–organic-frameworks (MOFs).[42]

Conclusions

In conclusion, we have demonstrated the phosphate-addition induced improvement of the synthesis yield of fumarate from CO_2 and pyruvate in an aqueous medium using a multi-biocatalytic system of ME from *Sulfobus tokodaii* and FUM from porcine heart in the presence of NADH. Focusing on the subunit structure of FUM, we attempted to improve the production of fumarate based on the dehydration of L-malate by saturating the additional substrate binding site of FUM with phosphate. Under the reaction conditions of L-malate (1.0 mM) and FUM (1.3 nM) in HEPES buffer (pH 7.0) for fumarate production, the addition of 70 mM phosphate improved the fumarate production rate up to 2.4 times compared to no addition of phosphate. In particular, the conversion yield for pyruvate and bicarbonate to fumarate with the system of ME and FUM was improved up to 1.6 times due to the improvement in the catalytic activity of FUM caused by the addition of phosphate in this system.

Conflicts of interest

There are no conflicts to declare.

Acknowledgements

This work was partially supported by Grant-in-Aid for Scientific Research (B) (22H01872) and Fund for the Promotion of Joint International Research (Fostering Joint International Research (B)) (19KK0144).

Notes and references

1 Y. Jiang, A. J. J. Woortman, G. O. R. Alberda van Ekenstein and K. Loos, *Polym. Chem.*, 2015, **6**, 5451.
2 A. Pellis, A. E. Herrero, L. Gardossi, V. Ferrario and G. M. Guebitz, *Polym. Int.*, 2016, **65**, 861.
3 N. A. Rorrer, J. R. Dorgan, D. R. Vardon, C. R. Martinez, Y. Yang and G. T. Beckham, *ACS Sustainable Chem. Eng.*, 2016, **4**, 6867.
4 B. D. Ahn, S. H. Kim, Y. H. Kim and J. S. Yang, *J. Appl. Polym. Sci.*, 2001, **82**, 2808.
5 I. Bechthold, K. Bretz, S. Kabasci, R. Kopitzky and A. Springer, *Chem. Eng. Technol.*, 2008, **31**, 647.
6 R. M. Deshpande, V. V. Buwa, C. V. Rode, R. V. Chaudhari and P. L. Mills, *Catal. Commun.*, 2002, **3**, 269.
7 D. Minh, M. Besson, C. Pinel, P. Fuertes and C. Petitjean, *Top. Catal.*, 2010, **53**, 1270.
8 N. Jacquel, F. Freyermouth, F. Fenouillot, A. Rousseau, J. P. Pascault, P. Fuertes and R. Saint-Loup, *J. Polym. Sci., Part A: Polym. Chem.*, 2011, **49**, 5301.
9 J. Shao, Y. Ni and L. Yan, *J. Bioresour. Bioprod.*, 2021, **6**, 39.
10 W. J. Landsperger and B. G. Harris, *J. Biol. Chem.*, 1976, **251**, 3599.
11 J. A. Milne and R. A. Cook, *Biochemistry*, 1979, **18**, 3605.
12 N. Yumoto and M. Tokushige, *Biochem. Biophys. Res. Commun.*, 1988, **153**, 1236.
13 S. Beeckmans and L. Kanarek, *Eur. J. Biochem.*, 1977, **78**, 437.
14 M. Mescam, K. Vinnakota and D. Beard, *J. Biol. Chem.*, 2011, **286**, 21100.
15 T. Mizobata, T. Fujioka, F. Yamasaki, M. Hidaka, J. Nagai and Y. Kawata, *Arch. Biochem. Biophys.*, 1998, **355**, 49.
16 J. S. Keruchenko, I. D. Keruchenko, K. L. Gladilin, V. Zaitsev and N. Y. Chiragadze, *Biochim. Biophys. Acta*, 1992, **1122**, 85.
17 J. C. Sacchettini, T. Meininger, S. Roderick and L. J. Banaszak, *J. Biol. Chem.*, 1986, **261**, 15183.
18 J. M. Lowenstein, Citric Acid Cycle, *Methods in Enzymology*, Academic Press, Boston, 1969, vol. 13.
19 L. Stryer, Citric acid cycle, in *Biochemistry*, W. H. Freeman and Company, New York, 4th edn, 1995.
20 S. J. Barnes and P. D. Weitzman, *FEBS Lett.*, 1986, **201**, 267.
21 S. Zhang and D. A. Bryant, *Science*, 2011, **334**, 1551.
22 J. M. Berg, J. L. Tymoczko and L. Stryer, The Citric Acid Cycle, *Biochemistry*, W. H. Freeman and Company, New York, 5th edn, 2002.
23 R. Ruppert, S. Herrmann and E. Steckhan, *Tetrahedron Lett.*, 1987, **28**, 6583.
24 E. Steckhan, S. Herrmann, R. Ruppert, J. Thömmes and C. Wandrey, *Angew. Chem., Int. Ed. Engl.*, 1990, **29**, 388.
25 H. C. Lo, O. Buriez, J. B. Kerr and R. H. Fish, *Angew. Chem., Int. Ed.*, 1999, **38**, 1429.
26 H. C. Lo, C. Leiva, O. Buriez, J. B. Kerr, M. M. Olmstead and R. H. Fish, *Inorg. Chem.*, 2001, **40**, 6705.
27 C. L. Pitman, O. N. L. Finster and A. J. M. Miller, *Chem. Commun.*, 2016, **52**, 9105.
28 R. Ruppert, S. Herrmann and E. Steckhan, *J. Chem. Soc., Chem. Commun.*, 1988, 1150.
29 J. Canivet, G. Süss-Fink and P. Štěpnička, *Eur. J. Inorg. Chem.*, 2007, **2007**, 4736.
30 D. Sivanesan and S. Yoon, *Polyhedron*, 2013, **57**, 52.
31 F. Hildebrand, C. Kohlmann, A. Franz and S. Lütz, *Adv. Synth. Catal.*, 2008, **350**, 909.
32 T. Katagiri and Y. Amao, *New J. Chem.*, 2021, **45**, 15748.
33 T. Katagiri, Y. Kita and Y. Amao, *Catal. Today*, 2022, DOI: **10.1016/j.cattod.2022.04.018**, in press.
34 T. Katagiri and Y. Amao, *Sustainable Energy Fuels*, 2022, **6**, 2581.
35 M. Takeuchi and Y. Amao, *React. Chem. Eng.*, 2022, **7**, 1931.
36 Y. Morimoto, K. Honda, X. Ye, K. Okano and H. Ohtake, *J. Biosci. Bioeng.*, 2014, **117**, 147.
37 J. C. Sacchettini, M. W. Frazier, D. C. Chiara, L. J. Banaszak and G. A. Grant, *Biochem. Biophys. Res. Commun.*, 1988, **153**, 435.
38 S. Beeckmans and E. Van Driessche, *J. Biol. Chem.*, 1998, **273**, 31661.
39 T. Weaver and L. Banaszak, *Biochemistry*, 1996, **35**, 13963.
40 R. Morellon-Sterling, D. Carballares, S. Arana-Peña, El-H. Siar, S. A. Braham and R. Fernandez-Lafuente, *ACS Sustainable Chem. Eng.*, 2021, **9**, 7508.
41 R. A. Sheldon and S. van Pelt, *Chem. Soc. Rev.*, 2013, **42**, 6223.
42 M. Chai, S. Razavi Bazaz, R. Daiyan, A. Razmjou, M. Ebrahimi Warkiani, R. Amal and V. Chen, *Chem. Eng. J.*, 2021, **426**, 130856.